Available online at www.sciencedirect.com
ScienceDirect
Catalysis Today 118 (2006) 214–222
CATALYSIS TODAY
www.elsevier.com/locate/cattod

Steam reforming of methane in equilibrium membrane reactors for integration in power cycles

A. Bottino [a], A. Comite [a,*], G. Capannelli [a], R. Di Felice [b], P. Pinacci [c]

[a] *Department of Chemistry and Industrial Chemistry, Via Dodecaneso 31, 16146 Genoa, Italy*
[b] *Department of Process and Chemical Engineering "G. Bonino", Via Opera Pia 15, Genoa, Italy*
[c] *CESI, Via Rubattino 54, 20134 Milano, Italy*

Abstract

Methane steam reforming is the most important industrial route to produce H_2. The process is governed by equilibrium reactions, the overall process is endothermic and high temperatures are required to reach satisfactory methane conversions. The possibility of using a membrane reactor, which separates H_2 from the reaction zone with a subsequent improvement of the conversions, is a challenge of many academic and industrial researchers. A great effort of membrane reactor analysis applied to steam reforming is necessary in the light of the novel and potential process applications (fuel cells, CO_2 capture).

This paper presents the model of a non-adiabatic methane steam reformer membrane reactor (MSRMR) working in equilibrium conditions. The model was used to investigate the effects of some variables (e.g. temperature profile, separation efficiency, plant size) on the membrane area and the energy required by the process, which in turn affect fixed and operating costs.

The simulations showed that the membrane area required sharp increases in the reactor size and that for large plants the development of thin and permeable membranes is a key issue.

Keywords: Methane steam reforming; Pd membrane; Membrane reactors

1. Introduction

Methane steam reforming (MSR) is a widely studied process because of its importance for hydrogen production. In the past, the majority of the studies were devoted to the application and the optimisation of this process for the production of synthesis gas to be used in the chemical industry (e.g. ammonia production).

Methane steam reforming is an endothermic process limited by equilibrium. A great effort is currently being carried out to study MSR using membrane reactors (MRs) to improve the process yield. The role of the membrane is the removal of hydrogen from the reaction side to shift the equilibrium conversion to higher values.

New emerging technologies, as well as fuel cells and the necessity to reduce CO_2 emissions, have focussed on the application of steam reforming to produce H_2 for power applications [1–3].

The use of a membrane coupled to a steam reformer opens new, interesting and potential applications, e.g. in fuel cell systems and power generation plants with CO_2 capture. Fig. 1 reports a simplified scheme of a potential cycle, which generates electrical power by integrating a membrane steam reformer and a fuel cell system. The main advantage is clearly the production of "clean electrical power" with low emissions (especially CO_2 that can be easily captured in a rich stream). Similarly, the membrane steam reactor should be integrated in power cycles with power generation by turbines, again with the aim to produce power energy with low emissions [1,4,5].

Methane steam reforming in a membrane reactor has been studied in different reactor configurations (co-current and counter-current fixed bed, fluidised bed, etc.) in the presence of a catalyst both experimentally and modelled in kinetic conditions [6–8]. Little literature can be found on the analysis of the membrane reactor for methane steam reforming in

---

* Corresponding author. Tel.: +39 010 3538719; fax: +39 010 3538733.
E-mail address: acomite@chimica.unige.it (A. Comite).

0920-5861/$ – see front matter © 2006 Elsevier B.V. All rights reserved.
doi:10.1016/j.cattod.2005.11.095

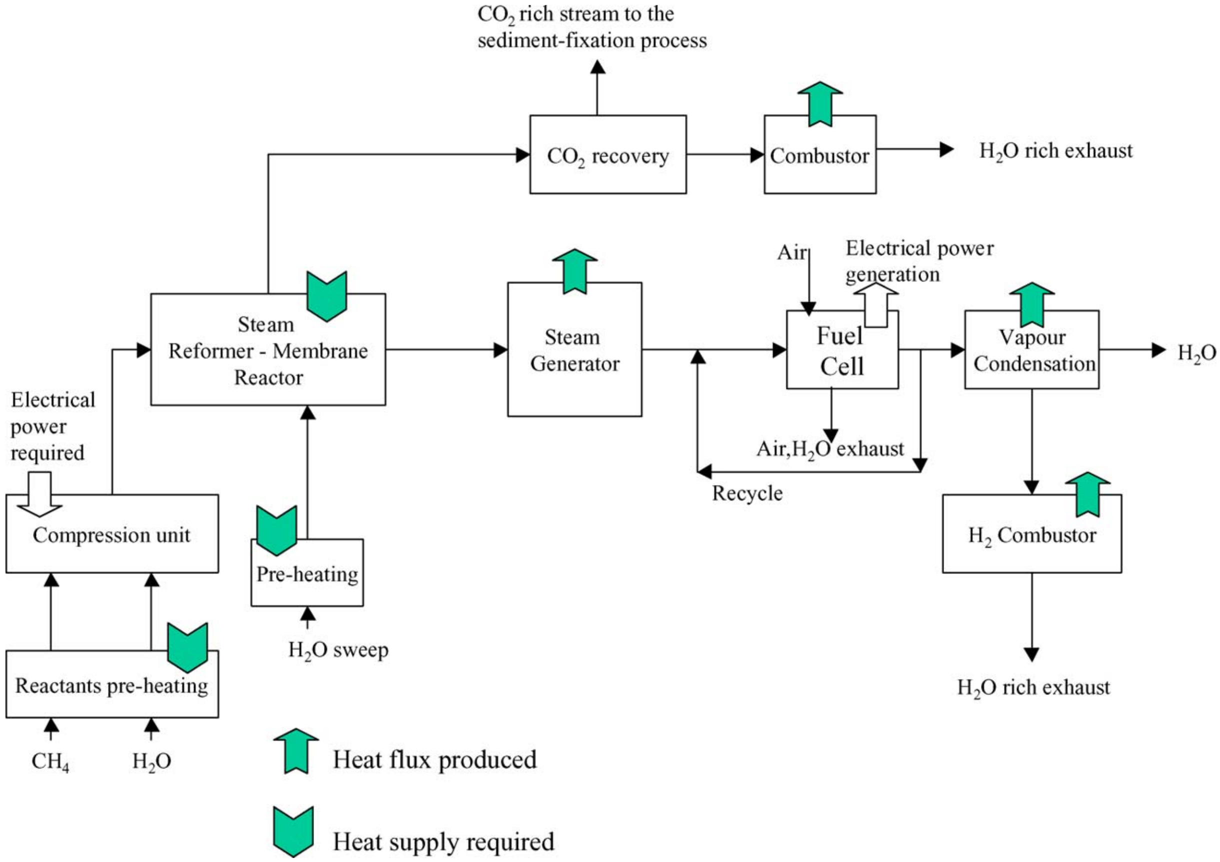

Fig. 1. Scheme of a potential application of MRSMR in a cycle to generate electrical power by fuel cells with low CO_2 emissions.

equilibrium conditions [9,10]. Nevertheless, the model reported does not give any sustainable indication (e.g. membrane area, energy requirement) for economic and efficiency evaluation of the membrane reactors integration in other process cycles. In commercial reformers the reaction conditions lead to a product composition, which is usually very close to the equilibrium of the methane reforming reaction and of the shift reaction [11]. Subsequently, simple models that simulate the equilibrium conditions for the membrane steam reactor are necessary in order to be integrated with larger process models, to economically simulate and evaluate novel applications like integrated fuel cell or turbine power cycles. Following this direction Jordal et al. [4] developed a simple model methane steam reforming membrane reactor (MSRMR) constituted of many equilibrium-separation stages (with the sweep gas in counter-current configuration). They compared the dense membrane performance with the microporous one in a MSRMR integrated in a gas turbine power cycle aimed at the CO_2 capture. In this case also no detailed results about the MSRMR were shown.

This paper presents a model of a non-adiabatic methane steam reformer membrane reactor working in equilibrium conditions. The model was used to investigate the effects of some variables (e.g. temperature profile, separation efficiency, plant potentiality) on the membrane area and the energy required by the process, which in turn affects fixed and operating costs of the plant.

2. Model

2.1. Model description, equations and material balances

The approach used to model the reactor is similar to that reported by Johannessen and Jordal [5] and shown in Fig. 2. The key equations are reported in Table 1. The methane steam reforming membrane reactor was conceived as made up of several stages (n) in cascade. In each stage a feeding stream, which contains the reactants (CH_4, H_2O_{vap} and CO), goes into the reaction chamber (R) where the methane steam reforming and water gas shift reactions occur in isothermal conditions. The following reactions were considered in detail:

(a) methane–steam reforming reaction

$$CH_4 + H_2O \Leftrightarrow CO + 3H_2, \quad \Delta H^\circ_{sr} = 206\,\text{kJ/mol}$$

the reaction is endothermic and the equilibrium composition of this reaction is pressure dependent (Eq. (a) in Table 1).

(b) water–gas shift reaction (WGS)

$$CO + H_2O \Leftrightarrow CO_2 + H_2, \quad \Delta H^\circ_{wgs} = -41\,\text{kJ/mol}$$

The WGS reaction is slightly exothermic (see Eq. (b) in Table 1).

The process where both reactions are considered is globally endothermic (165 kJ/mol) and subsequently a certain amount of heat (depending on the extent of each reaction) has to be

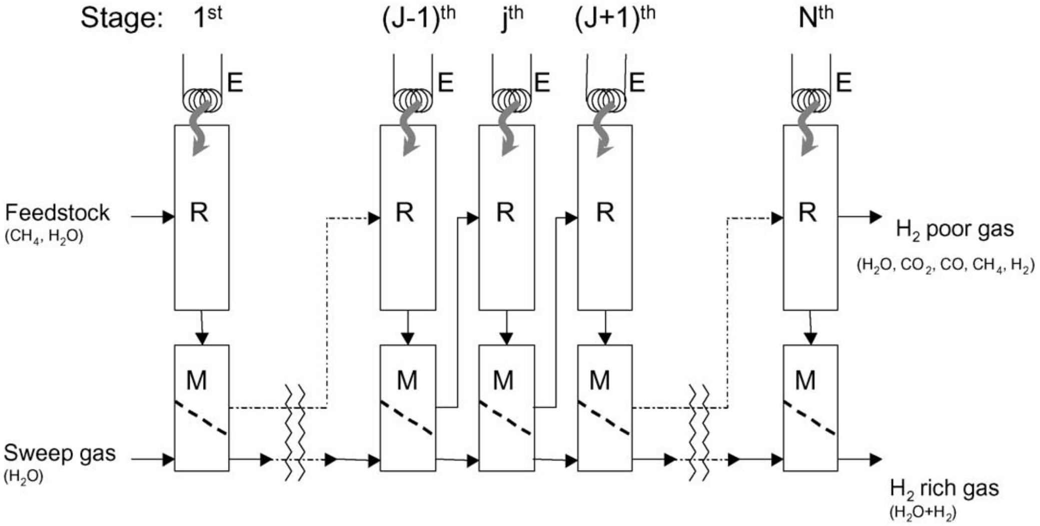

Fig. 2. Outline of the model of the MSRMR. R: reaction chamber; M: membrane; E: heat exchanger.

supplied to the system. The temperature dependence of the equilibrium constants $K_{p_{\mathrm{sr}}}$ and $K_{p_{\mathrm{wgs}}}$ was estimated using the correlations from Hou and Hughes [12] (Eqs. (c) and (d) in Table 1).

Component E in chamber R represents a system (e.g. an exchanger or a flame) supplying the required amount of energy to each stage.

The stream in exit from reaction chamber R meets a membrane, which is selective only to H_2. Then H_2 is separated with a certain efficiency (σ) and the poor H_2 stream goes into the next stage and the rich H_2 stream joins the others of the same kind. Both reactions are governed by the equilibrium and the removal (by permeation through a membrane) of one of the products (e.g. hydrogen) could shift the equilibrium towards a higher conversion of methane in the subsequent stage. The permeation of H_2 through a membrane could result in the possibility of using lower temperatures with the minimisation of side reactions like carbon formation, for example. Perfect mixing is assumed in the reaction chambers (R) and in the permeators (M).

The permeation of H_2 from the reaction zone can be obtained using metallic membranes formed by Pd or its alloys. Unless otherwise specified the permeation characteristics of the membrane are described by Richardson's equation with the parameters found by Morreale et al. [13] and reported in Table 1 (Eqs. (e) and (f)). The H_2 flow in each stage across the membrane $n_{H_2,j}$ is linked to the H_2 separation efficiency, σ, the membrane area in the considered stage and the H_2 flux through the membrane material by Eq. (g) in Table 1. The total membrane surface area required is the sum of the membrane area in the single stages.

The total methane conversion and the methane conversion in each stage are defined by Eqs. (h) and (i), respectively.

From a thermal point of view the MSRMR is non-adiabatic and subsequently it can exchange heat both with the environment or in a controlled manner with a system maintaining the temperature at desired values. In each stage the heat supplied, coupled with the reaction heat required by the chemical process at the conversion reached at that stage, determines the temperature. In other words, once the temperature profile has been fixed along the whole reactor at each stage, it is possible to calculate the amount of heat that should be supplied to each stage. Eq. (l) shows the relation among the temperature in each stage, the heat supplied and the conversion of the two reactions taking part in the process. The total heat flow required is the sum of each heat flow required in the single stages. The molar heat capacity *Cp* of each gas and the reaction enthalpies were expressed using a fourth temperature power law (Eqs. (m)–(s) in Table 1).

To summarize, the main model assumptions are:

- The MSRMR is a train of single isothermal stages where the equilibrium composition is established in a reaction chamber at the stage temperature. On the whole, the MSRMR is non-adiabatic because it can exchange heat with an external source (each stage can have a different temperature depending on the heat exchanged and on the partial conversions achieved in each stage).
- In the reaction chambers it is assumed that the equilibrium composition will take place. This fact states that the phenomena which keeps a system out of equilibrium conditions are not taken into consideration (fluidynamic, heat and mass transfer limitations). In each single part of the MSRMR perfect mixing is assumed. In actual steam reforming plants the gas composition obtained is very close to that expected from equilibrium calculations [11,16].
- In order to study the MSRMR performance a membrane with similar characteristics to those of a Pd membrane are considered. Pd membranes are already available on the market and although they present some drawbacks (e.g. embrittlement owing to phase changes, difficulty in obtaining very H_2 selective thin membranes) and other materials currently studied are available (alloys, metal–ceramic composites) with better performances, the simulation carried out using the permeation characteristics of the Pd membrane can give an idea of the performances that we can expect from an MSRMR.

Table 1
Main equations used to model the Methane steam reforming membrane reactor

Equation	Notes	Equation	Notes
$K_{p_{\mathrm{sr}}} = \left\{ \frac{y_{\mathrm{CO}} y_{\mathrm{H_2}}^3}{y_{\mathrm{CH_4}} y_{\mathrm{H_2O}}} \right\}_{\mathrm{eq}} P^2$	Equilibrium constant and composition for the MSR reaction	$x_{\mathrm{CH_4}}^j = \frac{n_{\mathrm{CH_4}}^{j-1} - n_{\mathrm{CH_4}}^j}{n_{\mathrm{CH_4}}^{j-1}}$	CH_4 conversion between two consecutive stages
$K_{p_{\mathrm{wgs}}} = \left\{ \frac{y_{\mathrm{CO_2}} y_{\mathrm{H_2}}}{y_{\mathrm{CO}} y_{\mathrm{H_2O}}} \right\}_{\mathrm{eq}}$	Equilibrium constant and composition for the WGS reaction	$x_{\mathrm{CH_4}} = \frac{n_{\mathrm{CH_4}}^0 + \sum_1^N (n_{\mathrm{CH_4}}^{j-1} x_{\mathrm{CH_4}}^j)}{n_{\mathrm{CH_4}}^0}$	Overall CH_4 conversion at the *j*thstage
$K_{p_{\mathrm{sr}}} = 1.198 \times 10^{13}\, \mathrm{e}^{(-26{,}830/T)}$	Dependence of the equilibrium constant for the MSR on the temperature	$T_j - T_{j-1} = \frac{q_j - x_{\mathrm{CH_4},j}\, \Delta H_{\mathrm{MSR}} - x_{\mathrm{CO},j}\, \Delta H_{\mathrm{wgs}}}{C_{p,j}}$	Energy balance at the *j*th stage
$K_{p_{\mathrm{wgs}}} = 1.767 \times 10^{-2}\, \mathrm{e}^{(-4400/T)}$	Dependence of the equilibrium constant for the WGS reaction on the temperature	$\frac{K_{p_{\mathrm{sr}}}}{P^2} = \frac{(n_{\mathrm{CO},j-1} + \alpha - \beta)\,(n_{\mathrm{H_2},j-1} + 3\alpha + \beta)^3}{(n_{\mathrm{CH_4},j-1} - \alpha)\,(n_{\mathrm{H_2O},j-1} - \alpha - \beta)\,(n_{\mathrm{tot},j-1} + 2\alpha)^2}$	Molar balances into the equilibrium constant equation for the MSR reaction
$N_{\mathrm{H_2}} = \frac{k}{t}\,(p_{\mathrm{H_2},C}^n - p_{\mathrm{H_2},P}^n)$	Richardson's equation to describe the H_2 flux through a Pd membrane	$K_{p_{\mathrm{wgs}}} = \frac{(n_{\mathrm{CO_2},j-1} + \beta)\,(n_{\mathrm{H_2},j-1} + 3\alpha + \beta)}{(n_{\mathrm{CO_2},j-1} + \alpha - \beta)\,(n_{\mathrm{H_2O},j-1} - \alpha - \beta)}$	Molar balances into the equilibrium constant equation for the WGS reaction
$k = k_0\, \mathrm{e}^{(E_{\mathrm{diff}}/RT)}$	$k_0 = 1.97 \times 10^{-7}$ mol m^{-1} s^{-1} $Pa^{-0.5}$, $E_{\mathrm{diff}} = 13{,}810$ J/mol $n = 0.5$	$x_{\mathrm{CH_4},j} = \frac{\alpha}{n_{\mathrm{CH_4},j}}$	CH_4 conversion (see Eq. (h)) and the solution of the non-linear system
$n_{\mathrm{H_2},j} = \frac{A_j N_{\mathrm{H_2},j}}{\sigma}$	H_2 molar flow through the membrane vs. the membrane area and the separation efficiency	$x_{\mathrm{H_2O},j} = \frac{\alpha + \beta}{n_{\mathrm{H_2O},j}}$	H_2O conversion (see Eq. (i)) and the solution of the non-linear system
$Cp_{\mathrm{CH_4}} = 26.86 + 2.817 \times 10^{-3} T + 1.15 \times 10^{-4} T^2 - 9.451 \times 10^{-8} T^3 + 2.374 \times 10^{-11} T^4$			
$Cp_{\mathrm{H_2O\,vap}} = 33.20 - 4.494 \times 10^{-3} T + 2.286 \times 10^{-5} T^2 - 1.243 \times 10^{-8} T^3 + 2.252 \times 10^{-12} T^4$			
$Cp_{\mathrm{CO}} = 31.3 - 1.699 \times 10^{-2} T + 4.053 \times 10^{-5} T^2 - 2.834 \times 10^{-8} T^3 + 6.686 \times 10^{-12} T^4$			
$Cp_{\mathrm{H_2}} = 26.78 + 1.224 \times 10^{-2} T - 2.299 \times 10^{-5} T^2 + 1.94 \times 10^{-8} T^3 - 5.261 \times 10^{-12} T^4$			
$Cp_{\mathrm{CO_2}} = 19.29 + 7.756 \times 10^{-2} T - 6.818 \times 10^{-5} T^2 + 3.175 \times 10^{-8} T^3 - 6.123 \times 10^{-12} T^4$			
$\Delta H_{\mathrm{sr}} = 190 + 5.90 \times 10^{-2} T - 1.36 \times 10^{-5} T^2 - 1.69 \times 10^{-8} T^3 + 6.6 \times 10^{-12} T^4$			
$\Delta H_{\mathrm{wgs}} = -39.3 - 1.98 \times 10^{-2} T + 5.36 \times 10^{-5} T^2 - 3.90 \times 10^{-8} T^3 + 9.85 \times 10^{-12} T^4$			

Table 2
Molar balances to calculate the equilibrium composition in the *j*th stage

Chemical compound	Moles before the reactions	Moles at equilibrium
CH_4	$n_{CH4,j-1}$	$n_{CH4,j} = n_{CH4,j-1} - \alpha$
H_2O	$n_{H_2O,j-1}$	$n_{H_2O,j} = n_{H_2O,j-1} - \alpha$
CO	$n_{CO,j-1}$	$n_{CO,j} = n_{CO,j-1} + \alpha - \beta$
H_2	$n_{H_2,j-1}$	$n_{H_2,j} = n_{H_2,j-1} + 3\alpha + \beta$
CO_2	$n_{CO_2,j-1}$	$n_{CO_2,j} = n_{CO_2,j-1} + \beta$
Total moles	$n_{tot,j-1} = n_{CH_4,j-1} + n_{H_2O,j-1} + n_{CO,j-1} + n_{H_2,j-1} + n_{CO_2,j-1}$	$n_{tot,j} = n_{tot,j-1} + 2\alpha$

2.2. Equilibrium calculation and numerical solution of the model

Table 2 reports the molar balances for each chemical species in the *j*th stage. These material balances were combined with Eqs. (a) and (b) and two new Eqs. (t) and (u) were obtained. α and β are the roots of the two equations and they are directly related to the conversions in the *j*th stage by Eqs. (v) and (z). The system of the two Eqs. (t) and (u) is highly non-linear and Eq. (u) (representing the WGS reaction) has a discontinuity near the system solution. Two procedures were tested to solve the system. The only algorithm found to be able to efficiently solve the two equations as reported was the one proposed by Shacham [14]. The second procedure used was the continuous analog of Newton's method (CANM) by Abrashkevich and Puzynin [15]. In this latter case the two non-linear equations were re-written in terms of the conversions of CH_4 and CO, in order to limit the solution range between 0 and 1, and to give the solving algorithm a higher possibility of success. The system solutions were compared for congruity with the results obtained by Grotendorst and Dornseiffer [16] and an excellent agreement was found.

3. Results and discussion

By setting the separation efficiency to zero the model can be used to simulate the behaviour of a Methane steam reformer (MSR) made up of several equilibrium isothermal stages. Using this feature a temperature profile increasing from 773 K at the first stage with an increment of 80 K from stage to stage was assumed. At the sixth stage the final temperature was about 1140 K and the CH_4 conversion was almost 80. The CH_4 conversion reached was slightly higher than that reported for a real steam reformer, having similar inlet and outlet temperatures [11]. The behaviour of MSR was compared with the MSRMR behaviour working with the same temperature profile and with a H_2 separation membrane efficiency of 80%. The results in terms of total H_2 molar flow and CH_4 conversion are shown in Fig. 3A and B, respectively. The H_2 produced in the membrane presence is higher for the MSRMR than for the MSR. Similarly the CH_4 conversion reached in each stage is higher for the MSRMR.

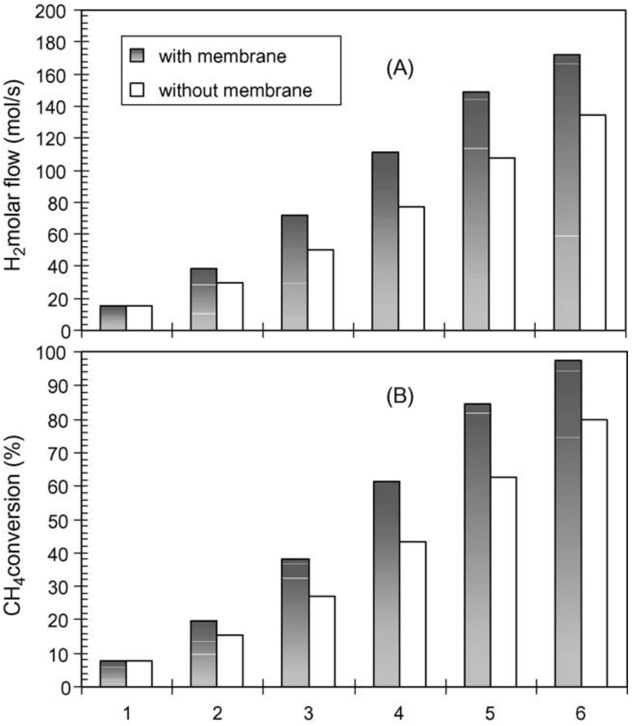

Fig. 3. Comparison between equilibrium conventional methane steam reformers and MSRMR. (A) Total H_2 produced in the single stages and (B) methane conversion. It was assumed a temperature profile increasing along the sequence of stages ($\Delta T/\Delta$stage = 80 K). T_{inlet} = 773 K, P = 20 bar, $m_{CH_4} = 3000\,kg/h$; $m_{H_2O} = 6000\,kg/h$; sweep side: P = 2 bar, $m_{H_2O} = 6000\,kg/h$. Pd membrane thickness = 30 μm; it is assumed that in each stage only 80% of the available H_2 permeates. Each point corresponds to a single stage.

The differences between the two reactors became more evident when the stages following the first one were considered. In the first stage, CH_4 and steam react in the reformer section (chamber R in Fig. 2) and the membrane removes H_2 with a separation efficiency set (80%). It is clear that in this stage the conversion level reached and the amount of H_2 produced in the two reactors should be the same. In the successive stages, the entering reactant stream has a lower content of H_2 in the MSRMR and subsequently the equilibrium composition of the MSRMR should be richer in H_2 than that of the MSR.

Fig. 4 shows the reactants and products distribution, the heat required and the membrane area necessary for each stage (each point in the plots represents a stage) against the CH_4 conversion for an MSRMR working in isothermal conditions. From Fig. 4A, CH_4 and H_2O in the reaction side are consumed by the equilibrium reactions, H_2 decreases in the reaction side (c) and increases in the permeate side because of the membrane presence. The production of CO_2 is higher than that of CO. In isothermal conditions the MSRMR obtains the highest CH_4 conversion in the first stage (Fig. 4B) corresponding to the highest heat supply (about 2.5 MW). The heat required at each stage decreases with an increase of the conversion in the successive stages, because the CH_4 conversion step between two consecutive stages is decreasing. While the membrane area necessary to separate H_2 with an efficiency of 80% is effectively increasing, it actually shows a plateau (which is slightly on the decrease) in the range of CH_4 conversion 30–60%. In the last stages, a higher membrane area is required, because of a lower driving force (the difference between the

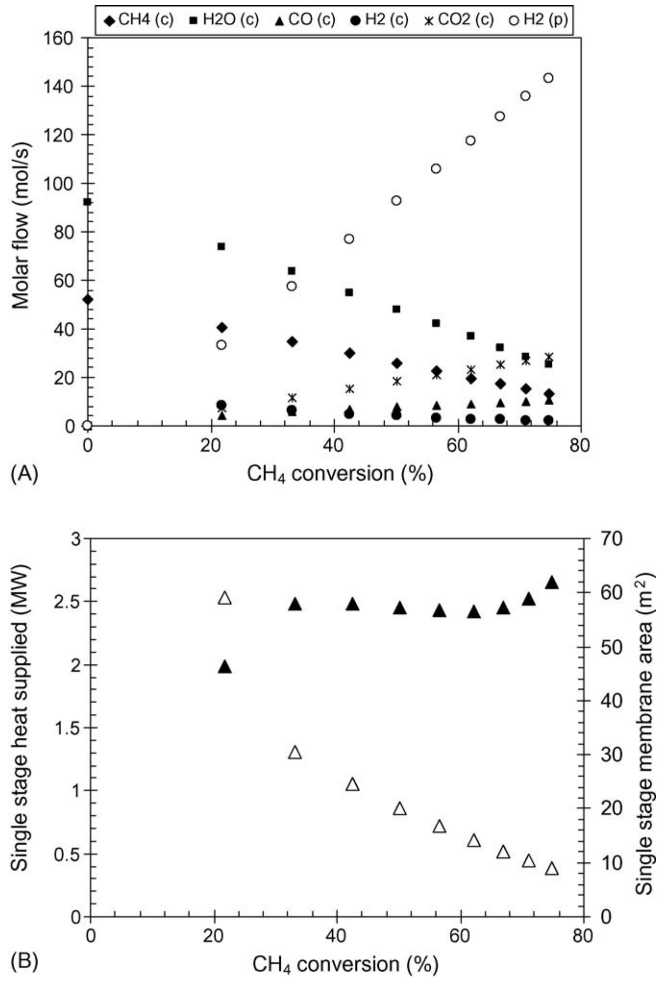

Fig. 4. (A) Molar flow of the species involved in the chemical reactions in the reaction side (c) and molar flow of H_2 (empty symbols) in the permeation side (p) as a function of CH_4 conversion and (B) heat supplied in each of the single stages and the corresponding membrane area as a function of the CH_4 conversion. $T_{stages} = 800$ K, $P = 20$ bar, $m_{CH_4} = 3000$ kg/h; $m_{H_2O} = 6000$ kg/h; sweep side: $P = 2$ bar, $m_{H_2O} = 6000$ kg/h. Pd membrane thickness = 30 μm; it is assumed that in each stage only 80% of the available H_2 permeates. Each point corresponds to a single stage.

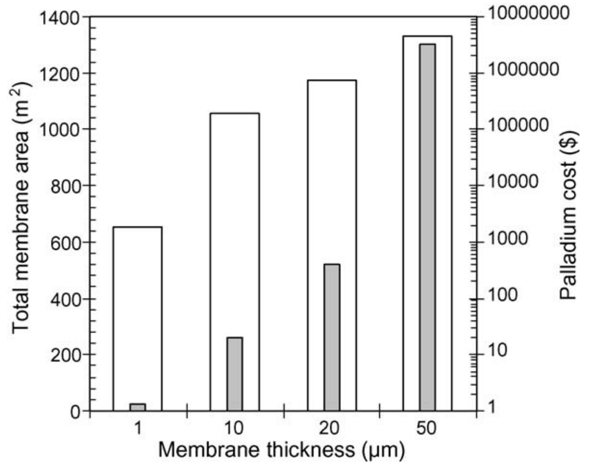

Fig. 5. Total membrane area required in the MSRMR and its cost expressed as Pd as a function of the membrane thickness. $T_{inlet} = 800$ K, all the stages have the same temperature, $P = 20$ bar, $m_{CH_4} = 3000$ kg/h; $m_{H_2O} = 6000$ kg/h; sweep side: $P = 2$ bar, $m_{H_2O} = 6000$ kg/h. It is assumed that in each stage only 80% of the available H_2 permeates. Grey bars on the left scale (total membrane area) and white bars on the right scale (palladium cost).

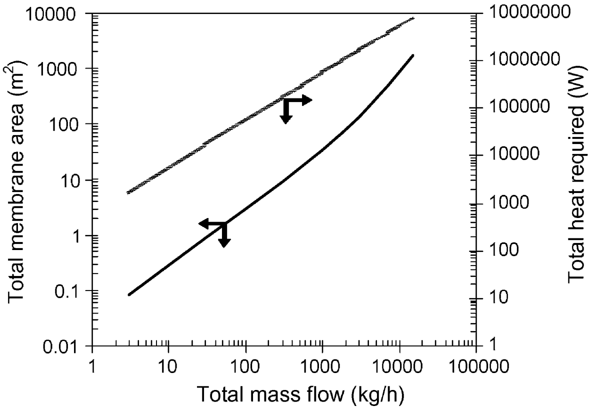

Fig. 6. Total membrane area required to reach a CH_4 conversion of 43.7% in nine stages as a function of the inlet total mass flow. $T_{inlet} = 900$ K, $P = 20$ bar, $m_{CH_4} = 1{-}5000$ kg/h; $m_{H_2O} = 6000$ kg/h; sweep side: $P = 2$ bar, $m_{H_2O} = 6000$ kg/h. Pd membrane thickness = 30 μm; it is assumed that in each stage only 80% of the available H_2 permeates.

square root of H_2 partial pressure in the reaction side and the one in the permeate side). Assuming that isothermal conditions for the MSRMR operations are adopted, although better temperature profiles will be shown, the influence of the membrane thickness on both the total membrane area for reaching the same CH_4 conversion (46.5%, after 10 stages) and the cost of the Pd quantity necessary is reported in Fig. 5. The higher the membrane thickness, the lower the H_2 flow through it, and the higher the membrane area necessary to accomplish the desired value of H_2 separation. The total cost of palladium (price of pure palladium from [17]) required to fulfil the plant specifications indicated in Fig. 5 greatly increases with the membrane thickness. It is clear that very thin membranes are preferable in order to significantly reduce the capital cost of the MSRMR plant. Pd membranes are available on the market as thin as 50 μm, but this is still insufficient for an MSRMR plant in order to be economically feasible. At laboratory scale many researchers have reported that it is possible to produce H_2 metal permeable membranes with very low thickness, better stability and long lifetime, maintaining the separation selectivity at high values, although further improvement in their production technology and engineering assembly as reactor is still to be done. Nevertheless, the use of MSRMR would be more realistic if integrated in small plants. This is shown in Fig. 6 where the total membrane area and the total heat required in an MSRMR plant as a function of the total mass flow of reactants is reported.

Fig. 7 depicts a design chart for an isothermal MSRMR working with a 30 μm Pd membrane. The design chart allows the calculation of the total membrane area necessary to obtain a certain level of CH_4 conversion for a given temperature. Each point represents a stage at the written temperature. Each continuous line represents an MSRMR reactor with all the stages at the same temperature. Higher temperatures favour the reactor to reach a higher CH_4 conversion under the same

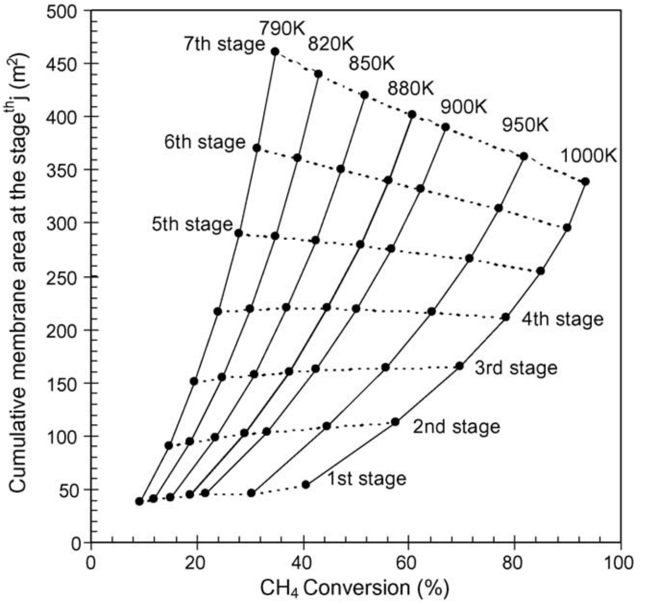

Fig. 7. Design chart for the MSRMR working in isothermal condition correlating the membrane area, the methane conversion and the temperature. $P = 20$ bar, $m_{CH_4} = 3000$ kg/h; $m_{H_2O} = 6000$ kg/h; sweep side: $P = 2$ bar, $m_{H_2O} = 6000$ kg/h. Pd membrane thickness = 30 μm; it is assumed that in each stage only 80% of the available H_2 permeates. Each point corresponds to a single stage.

Table 3
Output design data for the equilibrium membrane reactor

Temperature profile	Total membrane area (m^2)	Final CH$_4$ conversion (%)	Heat supplied (MW)
Decreasing profile	318.5	25.4	2.6
Isothermal profile	289.0	30.1	3.5
Increasing profile 1	268.7	42.2	5.5
Increasing profile 2	261.8	66.6	9.3
Increasing profile 3	251.5	97.8	14.1

For the operating condition refer to Fig. 8.

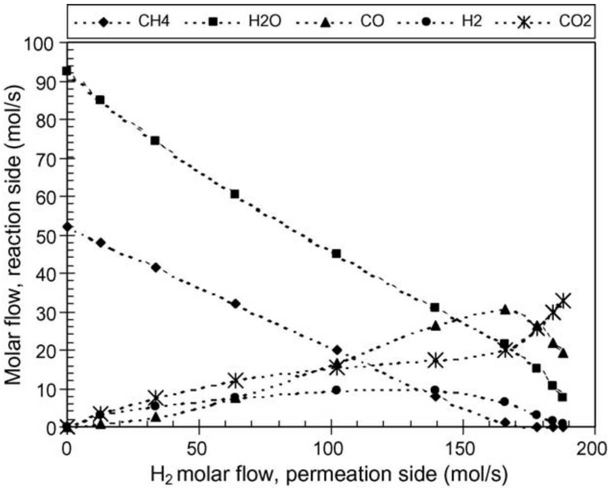

Fig. 9. Profiles of the molar flow of each component in the reaction side as a function of the H_2 molar flow in the permeation side. It was assumed a temperature profile increasing along the sequence of stages ($\Delta T/\Delta$stage = 80 K). $T_{inlet} = 773$ K, $P = 20$ bar, $m_{CH_4} = 3000$ kg/h; $m_{H_2O} = 6000$ kg/h; sweep side: $P = 2$ bar, $m_{H_2O} = 6000$ kg/h. Pd membrane thickness = 30 μm; it is assumed that in each stage only 80% of the available H_2 permeates. Each column of point corresponds to a single stage.

considered stage. At lower operating temperatures, the MSRMR requires a larger membrane surface area. If we consider the chart at each stage we can easily observe that the use of higher temperatures can be relevant at stages after the fourth, to decrease the membrane area and to reach higher conversions.

In the light of this last observation several temperature profiles were investigated for the MSRMR and the results are reported as a function of CH$_4$ conversion in Fig. 8, and in terms of total specifications (membrane area and total heat) in Table 3. The temperature profile reported versus the CH$_4$ conversion in Fig. 8B has a strong influence on the membrane area required in each single stage. A decreasing temperature profile obviously requires a higher membrane area for each successive stage, since the permeability of the membrane decreases with the decrease of the temperature. The MSRMR reactor operating with a decreasing temperature profile requires

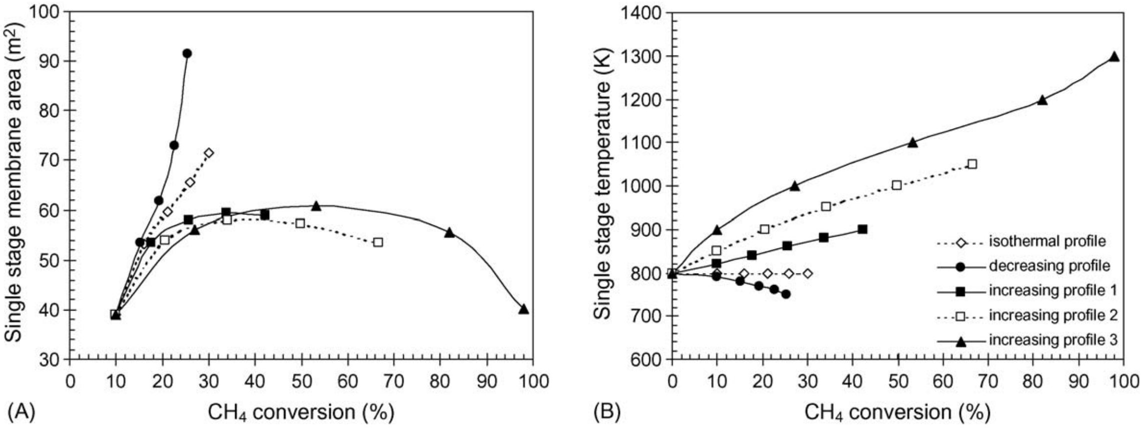

Fig. 8. (A) Membrane area required in each single stage vs. the total CH$_4$ conversion after the last stage and (B) temperature profiles used for the simulations. Operating conditions—reforming side: $T_{inlet} = 800$ K, $P = 20$ bar, $m_{CH_4} = 3000$ kg/h; $m_{H_2O} = 6000$ kg/h; sweep side: $P = 2$ bar, $m_{H_2O} = 6000$ kg/h. Pd membrane thickness = 30 μm; it is assumed that in each stage only 80% of the available H_2 permeates. Each point corresponds to a single stage.

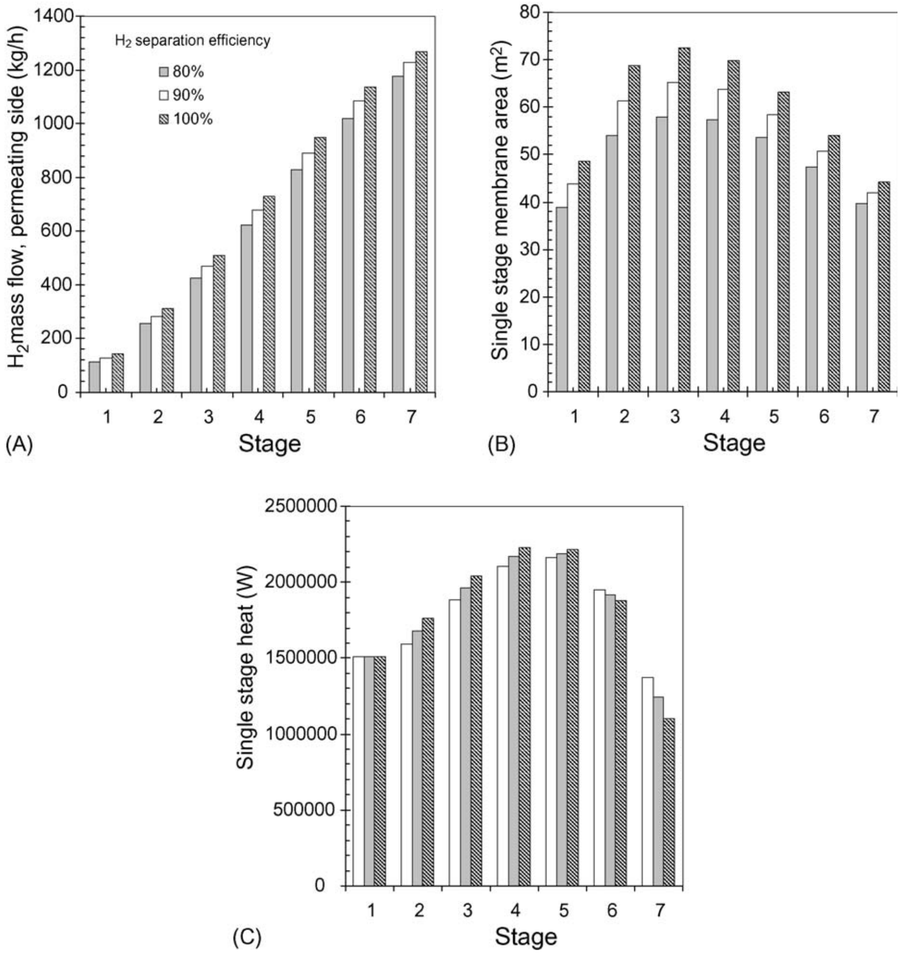

Fig. 10. Effect of the H_2 separation efficiency on the H_2 produced in the permeate side (A), on the single stage membrane area (B) and on the single stage heat supplied (C). It was assumed a temperature profile increasing along the sequence of stages ($\Delta T/\Delta$stage = 80 K). T_{inlet} = 773 K, P = 20 bar, $m_{CH_4} = 3000\,kg/h$; $m_{H_2O} = 6000\,kg/h$; sweep side: P = 2 bar, $m_{H_2O} = 6000\,kg/h$. Pd membrane thickness = 30 μm.

a minor flow of heat but lower CH_4 conversions are reached (Table 3). With an increasing temperature profile the membrane area required in each single stage grows at the beginning for low CH_4 conversion, reaches a maximum value (usually at the third stage) and then decreases. To explain more clearly this latter behaviour the composition of the gas mixture in the reactant side is reported in Fig. 9 against the H_2 molar flow in the permeate side. When the H_2 molar flow produced reaches about 165 mol/s, CH_4 is completely converted and the process carries on at the expense~~s~~ of the CO previously obtained through the reforming reaction of CH_4. The H_2 produced mainly through the water shift reaction is less and the membrane area needed to separate the H_2 tends to decrease, since the temperature at which the separation is carried out is higher.

Finally, the effect of the separation efficiency is shown in Fig. 10. A non-isothermal temperature profile was adopted to better show the differences. A higher H_2 separation efficiency leads to an increase of H_2 in the permeate side (Fig. 10A) because of the higher membrane area required (Fig. 10B). With the estimated temperature profile one can see that the major influence of the H_2 separation efficiency on the single stage membrane area is at the stages 2–4. Fig. 10C reports the heat supplied in each single stage. The sixth and seventh stages working with the higher efficiency require~~s~~ less heat, the reasons being already given above; from these stages the amount of CH_4 and of Co is sufficient to obtain a process, where the H_2 production is mainly governed by the exothermic WGS reaction.

4. Conclusions

Methane steam reforming in equilibrium conditions was considered in the presence of a Pd membrane for separating hydrogen. The system was designed as formed by a certain number of stages were the reaction reaches equilibrium and subsequently part of the hydrogen produced is removed by the Pd membrane. The model was formulated with the objective of designing an equilibrium membrane reactor obtaining the conversion, the membrane area and the energy consumption as final output.

The model showed that the temperature profile in the MSRMR plays an important role in the process economy (membrane area and heat supply).

Further investigations are being carried out in order to study the different parameters that influence the process with the aim to optimise them, to minimise the total reactor cost (minimum energy consumption and minimum membrane area) and its implementation in a power cycle.

Acknowledgement

The financial support of the Italian Authority of Energy is gratefully acknowledged (DM MICA 26.01.2000).

References

[1] R. Bredesen, K. Jordal, O. Bolland, High-temperature membranes in power generation with CO_2 capture, Chem. Eng. Process. 43 (2004) 1129–1158.

[2] J. Godat, F. Marechal, Optimization of a fuel cell system using process integration techniques, J. Power Sources 118 (2003) 411–423.

[3] S. Vasileiadis, Z. Ziaka-Vasileiadou, Efficient catalytic reactors-processors for fuel cells and synthesis applications, Sep. Purif. Technol. 34 (2004) 213–225.

[4] K. Jordal, R. Bredesen, H.M. Kvamsdal, O. Bolland, Integration of H_2-separating membrane technology in gas turbine processes for CO_2 capture, Energy 29 (2004) 1269–1278.

[5] E. Johannessen, K. Jordal, Study of a H_2 separating membrane reactor for methane steam reforming at conditions relevant for power processes with CO_2 capture, Energy Convers. Manage. 46 (2005) 1059–1071.

[6] W. Yu, T. Ohmori, T. Yamamoto, A. Endo, M. Nakaiwa, T. Hayakawa, N. Itoh, Simulation of a porous ceramic membrane reactor for hydrogen production, Int. J. Hydrogen Energy 30 (2005) 1071–1079, and literature therein.

[7] F. Gallucci, L. Paturzo, A. Basile, A simulation study of the steam reforming of methane in a dense tubular membrane reactor, Int. J. Hydrogen Energy 29 (2004) 611–617, and literature therein.

[8] T. Tsuru, K. Yamaguchi, T. Yoshioka, M. Asaeda, Methane steam reforming by microporous catalytic membrane reactors, AlChE J. 50 (2004) 2794–2805, and literature therein.

[9] G. Marigliano, G. Barbieri, E. Drioli, Equilibrium conversion for a Pd-based membrane reactor. Dependence on the temperature and pressure, Chem. Eng. Process. 42 (2003) 231–236.

[10] G. Barbieri, G. Marigliano, G. Perri, E. Drioli, Conversion–temperature diagram for a palladium membrane reactor. Analysis of an endothermic reaction: methane steam reforming, Ind. Eng. Chem. Res. 40 (2001) 2017–2026.

[11] P. Häussinger, R. Lohmüller, A.M. Watson, Hydrogen, Ullmann's Encyclopaedia of Industrial Chemistry, fifth ed., vol. A13.

[12] K. Hou, R. Hughes, The kinetics of methane steam reforming over a Ni/α-Al_2O_3 catalyst, Chem. Eng. J. 82 (2001) 311–328.

[13] B.D. Morreale, M.V. Ciocco, R.M. Enick, B.I. Morsi, B.H. Howard, A.V. Cugini, K.S. Rothenberger, The permeability of hydrogen in bulk palladium at elevated temperatures and pressures, J. Membr. Sci. 212 (2003) 87–97.

[14] M. Shacham, Numerical solution of constrained non-linear equations, Int. J. Numer. Methods Eng. 23 (1986) 1455–1481.

[15] A. Abrashkevich, I.V. Puzynin, CANM, a program for numerical solution of a system of nonlinear equations using the continuous analog of Newton's method, Comput. Phys. Commun. 156 (2004) 154–170.

[16] J. Grotendorst, J. Dornseiffer, Computer-aided modelling and simulation of the thermodynamics of steam reforming, Math. Comput. Simul. 51 (2000) 451–471.

[17] June 2005 Report, http://www.platinum.matthey.com/publications/price_reports.html.